Is concrete a poromechanics material?-A multiscale investigation of poroelastic properties

Franz-Joseph Ulm, Georgios Constantinides, Franz Heukamp

Is concrete a poromechanics material? - A multiscale investigation of poroelastic properties

F.-J. Ulm, G. Constantinides and F. H. Heukamp
Massachusetts Institute of Technology, Cambridge, MA 02139, USA

ABSTRACT

There is an ongoing debate, in Concrete Science and Engineering, whether cementitious materials can be viewed as poromechanics materials in the sense of the porous media theory. The reason for this debate is that a main part of the porosity of these materials manifests itself at a scale where the water phase cannot be considered as a bulk water phase, but as structural water; in contrast to water in the gel porosity and the capillary porosity. The focus of this paper is two-fold: (1) to review the microstructure of cementitious materials in the light of microporomechanics theory by starting at the scale where physical chemistry meets mechanics, and which became recently accessible to mechanical testing (nanoindentation); (2) to provide estimates of the poroelastic properties (drained and undrained stiffness, Biot coefficient, Biot modulus, Skempton coefficient) of cementitious materials (cement paste, mortar and concrete) by means of advanced homogenization techniques of microporomechanics. This combined experimental-theoretical microporomechanics approach allows us to deliver a blueprint of the elementary poroelastic properties of all cementitious materials, which do not change from one cementitious material to another, but which are intrinsic properties. These properties result from the intrinsic gel porosity of low density and high density C-S-H, which yield a base Biot coefficient of $0.61 < b \leq 0.71$ and a Skempton coefficient of $B = 0.20 - 0.25$. While the base Biot coefficient decreases gradually at larger scales, because of the addition of non-porous solid phases (Portlandite, ..., aggregates), it is shown that the Skempton coefficient is almost constant over 3-5 orders of magnitude.

RÉSUMÉ

Une question divise encore la communauté scientifique au sujet de la nature des bétons : les bétons peuvent-ils être considérés comme des milieux poreux au sens de la théorie des milieux poreux ? Ce débat provient de la nature d'une partie de la porosité des bétons. Cette dernière se manifeste à une échelle où la phase aqueuse ne peut plus être considérée comme un simple fluide newtonien, mais comme une phase structurale, contrairement à la porosité capillaire ou celle du gel. L'objectif de cet article est double : (1) Décrire la microstructure des ciments sous l'angle de la théorie de la micro-poromécanique, en partant d'une échelle décrite à la fois par la physico-chimie et la mécanique, et qui est récemment devenue accessible aux tests mécaniques (nanoindentation) ; (2) Estimer les propriétés poroélastiques (élasticité drainée ou non drainée, coefficient de Biot, module de Biot, coefficient de Skempton) des matériaux dérivés du ciment (ciment, mortier et béton) à l'aide des techniques d'homogénéisation de la micro-poromécanique. Cette approche micro-poromécanique à la fois expérimentale et théorique nous permet de reconnaître une marque de fabrique de tous les ciments, qui ne change pas d'un matériau à l'autre, mais qui donne accès à leurs propriétés intrinsèques. Ces propriétés résultent de la porosité intrinsèque au gel des C-S-H à faible et forte densités, qui donnent un coefficient de Biot entre $b = [0,61\text{-}0,71]$, et un coefficient de Skempton $B = [0,20\text{-}0,25]$. Tandis que le coefficient de Biot diminue progressivement aux grandes échelles, en raison de la contribution des phases solides non poreuses (Portlandite, ..., granulats), le coefficient de Skempton est presque constant sur une plage de 3 a 5 ordres de grandeur.

1. INTRODUCTION

Is concrete a porous material? - Or more precisely: is concrete a poromechanics material, that can be described within the framework of the porous media theory? *I.e.* in terms of the constitutive equations of poromechanics, *e.g.*

the one of linear poroelasticity [1, 2],

$$\Sigma_m = K_{\text{hom}} E - bp \tag{1}$$

$$\phi - \phi_0 = bE + \frac{p}{N} \tag{2}$$

where $\Sigma_m = \frac{1}{3}\Sigma : \mathbf{1}$ = the macroscopic mean stress, p = pore pressure; $E = \mathrm{E} : \mathbf{1}$ = the volume strain; $\phi - \phi_0$ = the porosity change, K_{hom} = drained bulk modulus; b = Biot-Willis parameter; and N = Biot skeleton modulus.

The question we here raise is motivated by a long and ongoing discussion in Concrete Science and Engineering, with two schools of thought existing: one which considers that the deformation behavior of concrete, while being a porous material, is insufficiently described by the poromechanics approach, because the main porosity of these materials manifests itself at a scale where the water phase cannot be considered as a bulk water phase, but as structural water (*e.g.* [3-5]). Therefore, the effective stress concept as originally proposed by Terzaghi [6] for $b = 1$, and refined by Biot [1] through introduction of the effective pressure coefficient $\phi_0 \le b \le 1$, should certainly fail to describe the deformation behavior of such materials. The second school of thought has considered concrete as a poromechanics material, without necessarily distinguishing between nano-, micro- and macroporosity, and this for both saturated concrete [7-10], and unsaturated cement-based materials [11, 12]; through the classical micro-macro relations of poroelasticity:

$$b = 1 - \frac{K_{\text{hom}}}{k_s}; \frac{1}{N} = \frac{b - \phi_0}{k_s} \tag{3}$$

where K_{hom}/k_s = the drained bulk modulus-to-solid bulk modulus ratio; ϕ_0 = initial porosity. According to Berryman [13], relations (3) were first obtained by Gassman in 1951 [14] for the case of a microhomogeneous porous media, and by Brown and Korringa [15] and Rice [16] in 1975 for general porous media with multiple minerals as constituents. The application to concrete faces several difficulties; for one concrete is a highly heterogeneous material, with a heterogeneity which manifests itself at multiple scales, in form of different pore spaces and multiple minerals that build up the solid phase.

This makes it difficult to define a single solid bulk modulus k_s or a single porosity ϕ_0 for such materials. The large range of values for b and N that are currently in use for cement-based materials highlights the uncertainty of estimating the poroelastic properties of cementitious materials.

Recent progress in experimental and theoretical microporomechanics makes it possible today to upscale poroelastic properties from very fine scales of heterogeneous materials. As nanoindentation has provided an unprecedented access to micromechanical properties of the elementary phases of cementitious materials [17-19], it becomes possible to break down the complex microstructure of cementitious materials to the scale where cementitious materials do no more change –in a statistical sense– from one mix proportion to another. This scale has been traditionally the scale of cement chemistry investigations, ever since Powers and his colleagues at the Portland Cement Association [20] in the 50ies recognized the colloidal and gel-like properties of cement paste, and of the C-S-H[1] component in particular. At this scale, the morphology and the mechanical properties do no more change, being determined by the chemical formation process, which is deterministic by nature. With this scale in mind, it becomes possible to employ advanced homogenization techniques of microporomechanics that became recently available [21-23], and adapt them to meet the requirements of the multiscale microstructure of cementitious materials, starting at the scale where physical chemistry meets mechanics. The results of this challenging endeavor are estimates of the poromechanics properties of cementitious materials at multiple scales. This is in short the focus of this paper, and the way by which we want to address the question - whether (and to which extent) concrete is a poromechanics material.

2. ELEMENTS OF CONTINUUM MICROPOROMECHANICS APPLIED TO CEMENT-BASED MATERIALS

Concrete is a fairly complex heterogeneous composite material, with a random microstructure at different length scales ranging from the nanometer scale to the macroscopic decimeter scale. Continuum micromechanics offers a framework to address this heterogeneity. The underlying idea of continuum micromechanics is that it is possible to separate a heterogeneous material into phases with on-average constant material properties. The three elements of continuum micromechanics are [24]:

1. *Representation*, which deals with the geometrical description of the considered heterogeneous material system. Representation includes the identification of the different phases in a representative element volume V (r.e.v.), and their morphology. A phase, in the sense of continuum micromechanics, is not necessarily a material phase as used in physical chemistry, but a material domain that can be identified, at a given scale, with a homogeneous deformation state, that is with on-average constant material properties. The classical poromechanics theory is based on a two-phase representation of a porous medium as a solid-fluid composite. As we will see, such a representation falls short in representing a multi-scale porous material such as concrete.
2. *Localization*, which establishes the link between a macroscopic strain (or stress), prescribed at the boundary ∂V of the r.e.v., and the microscopic strain (or stress) in the individual (homogeneous) phases composing the r.e.v.
3. *Homogenization*, which is based on volume averaging over the r.e.v. of the constitutive relations defined at the scale of the phases. Homogenization delivers the macroscopic poroelastic properties of the r.e.v. as a

[1] *Cement chemistry notation: C = CaO, S = SiO_2, H = H_2O.*

function of the microscopic phase properties, their volume fractions, and their specific morphologies.

Application of these three elements to cement-based porous materials is detailed below.

2.1 Representation of the multiscale microstructure of cement-based porous materials

The heterogeneity of cement-based material manifests itself at different scales. For purpose of poromechanical analysis, the microstructure can be broken down into four elementary levels, as sketched in Figs. 1 and 2 [25, 26]. These scales are discussed below.

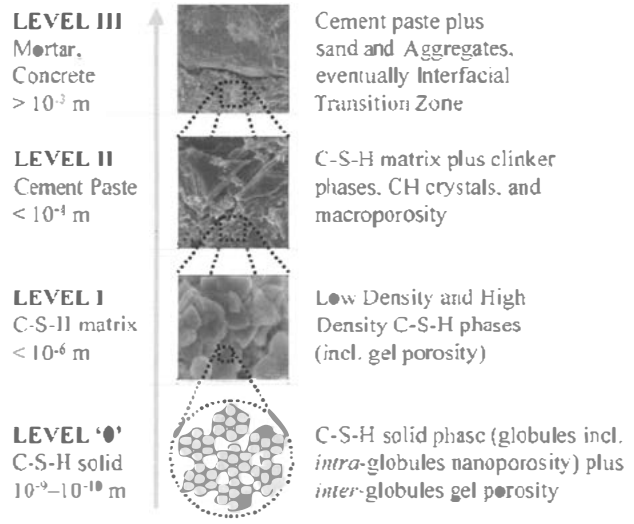

Fig. 1 - Representation of multiscale heterogeneous microstructure of cementitious composites (adapted from [25] and [29]).

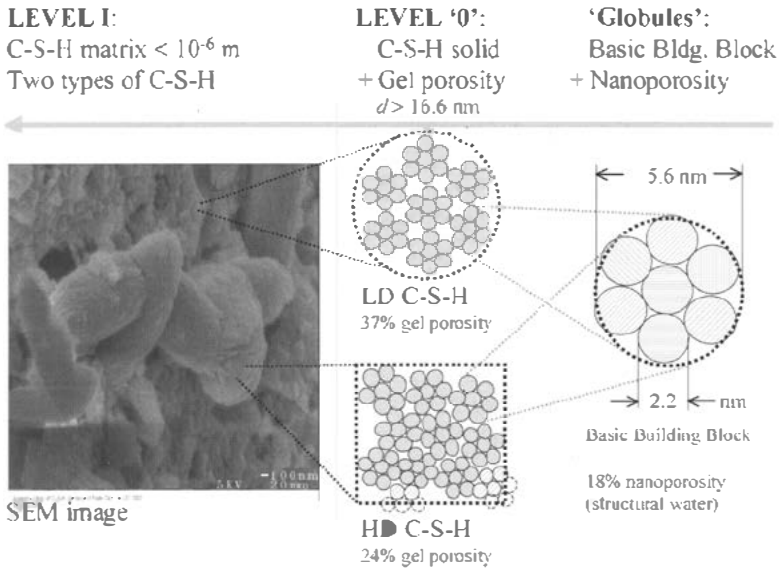

Fig. 2 - Level '0' C-S-H colloidal model of Jennings [29]: Gel porosity versus Nanoporosity.

2.1.1 *Level '0': Nanoscale*

The lowest level of a mechanical representation of the complex microstructure of cement-based materials is the largest scale at which the material properties do not change from one cement-based material to another. It is the scale, where physical chemistry meets mechanics; that is the material properties are solely defined by the physical chemistry of the formation process of the material. This scale is typically situated above the atomic scale. In the case of cement-based materials, it is the scale of the C-S-H solid that forms at early ages by the hydration of C_3S and C_2S. We refer to this scale as level '0', as explained below[2].

This scale has been the focus of many theoretical and experimental cement chemistry investigations, starting with the groundbreaking works of Powers and his colleagues at the Portland Cement Association [20] recognizing the colloidal and gel-like properties of the C-S-H component. Powers attributed a porosity of roughly 28% to this solid phase. Ever since, many models have been devised to characterize the microstructure with an emphasis on a layered structure of C-S-H. To cite a few, the well known Feldman-Sereda model postulated the existence of 'interlayer spaces' in the C-S-H gel, containing strongly adsorbed water [27]. Wittmann's Munich model is based on some of the concepts of colloidal science, relying particularly on the idea of a disjoining pressure that develops in the interlayer space as a consequence of hindered adsorption [3, 5]. Similar conclusions were arrived at by other authors as well (see *e.g.* [4]): given the characteristic size of the interlayer space of less than ten water molecules in size (elementary dimension of water is distance between O-atoms 0.284×10^{-9} m), it was quickly recognized that the water in this space cannot be considered to be a bulk water phase, to which *e.g.* Stokes equations apply. Instead, the mechanical response at this scale is dominated by the surface properties of the C-S-H gel, and the water present at this scale is structural water. Very recently, Jennings in a number of papers [28, 29], provided qualitative and quantitative evidence of an amorphous colloidal structure of the C-S-H, organized in 'globules' (see Fig. 2), composed of basic building blocks and an intra-globules porosity. This porosity which manifests itself at a scale smaller than the characteristic solid dimension of 2.2×10^{-9} m, is $\varphi_0 = 18\%$ irrespective of the type of C-S-H. Instead, it is intrinsic to the C-S-H solid phase, and can be associated with the nanoporosity filled by structural water (and not bulk water). Above this scale, there is a second type of porosity, the gel porosity, but which was found to differ from one type of C-S-H to another, as detailed below. Hence, from a poromechanics point of view, it is appropriate to consider this solid phase ('globules' in Jennings terminology) which includes a 18% intra-solid porosity filled by structural water, as the elementary solid phase of a poromechanics representation of cement-based materials. This solid phase has been found to be of a characteristic size of 5.6×10^{-9} m.

[2] *The name 'Level 0' for the nanoscale of C-S-H materials was coined by I.G. Richardson during the Gordon Conference on Cement-Based Materials in Ventura, Ca., March 7, 2002.*

2.1.2 *Level I: C-S-H phases - Gel Porosity - C-S-H matrix*

The solid phase of level '0' together with gel-porosity forms different types of C-S-H phases. These phases manifest themselves in units roughly larger than 16.6×10^{-9} m [29], as sketched in Fig. 2. We refer to this level as level I, as it represents the smallest material length scale that is presently accessible by mechanical testing, *i.e.* nanoindentation [19]. At level I, it is now well established that the C-S-H exists in at least two different forms, a low density (LD) and a high density (HD) form (see Fig. 2). The difference between the two types of C-S-H relates to the gel porosity of roughly 24% for HD-C-S-H, and 37% for LD-C-S-H [29], due to the different packing density of the C-S-H solid of the two types of C-S-H; in addition to the 18% nanoporosity within the C-S-H solid phase (at level '0'); see Fig. 2. In contrast to the nanoporosity, the gel porosity has a characteristic dimension of the solid phase, *i.e.* on the order of 5.6×10^{-9} m, in which the water present can be considered as a bulk water phase – in the sense of the poromechanics theory. The gel porosity can be defined in a standard manner:

$$\phi_0^{HD} = \frac{V_{f,HD}}{V_{HD}} = 0.24 \; ; \phi_0^{LD} = \frac{V_{f,LD}}{V_{LD}} = 0.37 \qquad (4)$$

where $V_{f,J}$ is the pore volume, and V_J the reference volume ($J = HD, LD$). The gel porosity values are also intrinsic to all cement-based materials: they are a consequence of the formation process of C-S-H in the course of hydration. That what changes from one cement paste material to the other is the volumetric proportion of HD-C-S-H and LD-C-S-H, within the C-S-H matrix. The overall porosity of a C-S-H matrix composed of the two porous material phases is:

$$\phi_0^{CSH} = \frac{V_{f,HD} + V_{f,LD}}{V_{CSH}} = f_{HD}\phi_0^{HD} + f_{LD}\phi_0^{LD} \qquad (5)$$

where $f_{HD} = V_{HD}/V_{CSH}$ and $f_{LD} = V_{LD}/V_{CSH} = 1 - f_{HD}$ stand for the volume fractions of the two types of C-S-H. In contrast to the intrinsic porosity values (4), the C-S-H matrix porosity (nanoporosity excluded) depends through the volume fractions on the mix proportions (and cement fineness [30]), and has the two limit cases $\phi_0^{HD} < \phi_0^{CSH} \leq \phi_0^{LD}$; for instance for a $w/c = 0.5$ cement paste, the volume ratio of HD and LD C-S-H is V_{HD}/V_{LD} =3:7 [28, 25]; thus $\phi_0^{CSH} = 0.33$. The ultimate mechanically intrinsic building blocks of C-S-H are the HD- and LD-C-S-H phases, for which the porosities do not change from one material to the other, nor the solid composition. This has been shown by nanoindentation tests by Acker [18] and Constantinides *et al.* [25, 19], who obtained the same stiffness values for the two types of C-S-H by nanoindentation of different cement-based materials (different *w/c*-ratio). These mean stiffness values are independent of the type of cementitious materials; instead they are intrinsic to cementitious materials in general; and that what changes from one to the other cementitious material is only the volume fractions of the HD-C-S-H and LD-C-S-H.

2.1.3 *Level II: Capillary porosity - n solid phases*

Level II refers to the cement paste, which manifests itself at a characteristic length scale of 10^{-6}-10^{-4} m (see Fig. 1). At this scale, the porous C-S-H matrix together with the unhydrated cement products (*i.e.* the four clinker phases C_3S, C_2S, C_3A, C_4AF), large Portlandite crystals ($CH = Ca(OH)_2$), aluminates and the macro-porosity ϕ_0 (which is often referred to as capillary porosity, and which is generally present only in high *w/c*-materials) form the cement paste. The porosity of a cement paste (excluding the nanoporosity), in which the water is a fluid phase in the sense of the poromechanics theory, is:

$$\phi_0^{II} = \phi_0 + f_{CSH}\phi_0^{CSH} = 1 - \sum_{r=1}^{n-1} f_r - (1 - \phi_0^{CSH}) f_{CSH} \qquad (6)$$

where $f_{CSH} = V_{CSH}/V_{II}$ is the volume fraction of the porous matrix, and $f_r = V_r/V_{II}$ is the volume fraction of the different solid phases. The solid volume fractions can be determined by advanced hydration models [30]. At this scale, the intrinsic phases (*i.e.* phases that do not change from one cement-based material to the other) are the four clinker phases, the Portlandite crystals, and the water phase saturating the pore space. Their material properties are well known by now thanks to nanoindentation: the stiffness values of the clinker phases have been determined by Velez *et al.* [17], the one of Portlandite crystals by Acker [18], and confirmed by Constantinides and Ulm [25]. From a morphological point of view, the composite cement paste consists of inclusions (clinker-phases, A-phase, CH-phase and porosity) embedded into a porous C-S-H matrix, which -at a level below- is composed of the two C-S-H-phases.

2.1.4 *Level III: Mortar and concrete*

Level III of a characteristic length scale greater than 10^{-3} m refers to mortar and concrete; that is a composite material composed of a porous cement paste matrix, and sand particle inclusions in the case of mortar, or aggregate inclusions in the case of concrete. Some authors consider in addition the Interfacial Transition Zone (ITZ) between inclusions and matrix, which has been focus of many micromechanical modeling attempts (*e.g.* [31-34]); but which will not be pursued further in this investigation. From a poromechanics point of view, the cement paste matrix is a porous matrix, while -except for special applications- any porosity contained in the aggregates is rather of occluded nature.

The intrinsic density, porosity and stiffness values of the different constituents of cement-paste materials over the range of length scales considered are summarized in Tables 1 and 2, and will serve as input parameter for the homogenization model of the poroelastic properties developed below. In this context, it is worth noting that the four levels described above respect the separability of scale condition; that is each scale is separated from the next one by at least one order of length magnitude. This is a prerequisite for the application of continuum micromechanics [24].

2.2 Localization

The breakdown of the multi-scale heterogeneous microstructure of cement-based materials into the four level

microstructure, separated on-average by one or several order of length magnitude, allows us to consider each level as a r.e.v., V, composed of n homogeneous phases (in a micromechanical sense) of constant material properties per phase (see Tables 1 and 2).

Following continuum micromechanics, each level is considered to be subjected to a homogeneous strain boundary condition of the Hashin type:

$$\text{on } \partial V : \boldsymbol{\xi}(\mathbf{x}) = \mathbf{E}\cdot\mathbf{x} \tag{7}$$

where $\boldsymbol{\xi}(\mathbf{x})$ is the microscopic displacement and $\mathbf{x}$ denotes the microscopic position vector.

Furthermore, the microscopic strain in the different phases is assumed to be linked to the macroscopic strain by a linear strain localization condition:

$$\boldsymbol{\varepsilon}(\mathbf{x}) = \mathbb{A}(\mathbf{x}) : \mathbf{E} \tag{8}$$

with $\mathbb{A}(\mathbf{x})$= the 4th order localization tensor, which satisfies the compatibility condition:

$$\mathbf{E} = \langle \boldsymbol{\varepsilon} \rangle_V \Leftrightarrow \langle \mathbb{A}(\mathbf{x}) \rangle_V = \mathbb{I} \tag{9}$$

where $\langle y \rangle_V = \frac{1}{V}\int y(\mathbf{x})\mathrm{d}V$ stands for the volume average of quantity y over domain V; and $\mathbb{I}$ is the 4th-order unit tensor. For a heterogeneous material composed of homogeneous phases, it is convenient to introduce a linear phase strain concentration of the form:

$$\langle \boldsymbol{\varepsilon} \rangle_{V_r} = \langle \mathbb{A}(\mathbf{x}) \rangle_{V_r} : \mathbf{E}; \sum_{r=1}^{n} f_r \langle \mathbb{A}(\mathbf{x}) \rangle_{V_r} = \mathbb{I} \tag{10}$$

where $f_r = V_r / V$ stands for the volume fraction of the phase. In the isotropic case, $\langle \mathbb{A}(\mathbf{x}) \rangle_{V_r}$ reduces to:

$$\langle \mathbb{A}(\mathbf{x}) \rangle_{V_r} = A_r^v \mathbb{J} + A_r^d \mathbb{K} \tag{11}$$

where A_r^v and A_r^d represent the volumetric and the deviatoric strain localization coefficient; $J_{ijkl} = \frac{1}{3}\delta_{ij}\delta_{kl}$ is the volumetric part of the 4th-order unit tensor $\mathbb{I}$, and $\mathbb{K} = \mathbb{I} - \mathbb{J}$ is the deviator part; δ_{ij} stands for the Kronecker delta.

The morphology encountered at all different levels of cement-based materials is of the Eshelbian-type, that is an ellipsoidal inclusion embedded in a reference medium [36], for which an estimate $\mathbb{A}_r^{est}$ of the localization tensor $\langle \mathbb{A}(\mathbf{x}) \rangle_{V_r}$ is given in the form [24]:

$$\mathbb{A}_r^{est} = [\mathbb{I} + \mathbb{S}_r^{Esh} : (\mathbb{C}_0^{-1} : \mathbb{C}_r - \mathbb{I})]^{-1} : \left\langle [\mathbb{I} + \mathbb{S}_r^{Esh} : (\mathbb{C}_0^{-1} : \mathbb{C}_r - \mathbb{I})]^{-1} \right\rangle_V^{-1} \tag{12}$$

where $\mathbb{C}_0$ is the tensor of elastic moduli of the reference medium, $\mathbb{C}_r$ is the 4th order stiffness tensor of phase $r = 1, n$; and $\mathbb{S}_r^{Esh}$ is the Eshelby tensor of phase r which depends on $\mathbb{C}_0$, the geometry and the orientation of phase r. According to the choice of the reference medium, one can distinguish: the Mori-Tanaka scheme, in which the reference medium is chosen to be the matrix phase (*i.e.* $\mathbb{C}_0 = \mathbb{C}_M$; the Self-Consistent Scheme, in which the homogenized medium is adopted as reference medium, that is $\mathbb{C}_0 = \mathbb{C}_{\text{hom}}$. In this application to cement-based materials, which are characterized at all levels by a dominating matrix phase, we will choose the Mori-Tanaka approximation [37]. Furthermore, given the random microstructure of cement-based materials, it is natural to consider all phases as isotropic and the inclusions as spherical. The first assumption implies the isotropy of the local and the reference medium, that is:

$$\mathbb{C}_r = 3k_r\mathbb{J} + 2g_r\mathbb{K}; \quad \mathbb{C}_0 = 3k_0\mathbb{J} + 2g_0\mathbb{K} \tag{13}$$

where k_r, g_r, k_0 and g_0 are the bulk moduli and the shear moduli of phase r and of the reference medium, respectively. The second assumption of spherical inclusions implies the following form of the Eshelby tensor $\mathbb{S}_r^{Esh}$ for phase r:

$$\mathbb{S}_r^{Esh} = \alpha_0^{est}\mathbb{J} + \beta_0^{est}\mathbb{K} \tag{14}$$

with

$$\alpha_0^{est} = \frac{3k_0}{3k_0 + 4g_0}; \quad \beta_0^{est} = \frac{6(k_0 + 2g_0)}{5(3k_0 + 4g_0)} \tag{15}$$

In this case, the localization tensor reduces to (11), in which the volumetric and deviatoric strain localization coefficients are estimated by:

$$A_r^{v,est} = \left(1 + \alpha_0^{est}\left(\frac{k_r}{k_0} - 1\right)\right)^{-1} \left[\sum_r f_r \left(1 + \alpha_0^{est}\left(\frac{k_r}{k_0} - 1\right)\right)^{-1}\right]^{-1} \tag{16}$$

$$A_r^{d,est} = \left(1 + \beta_0^{est}\left(\frac{g_r}{g_0} - 1\right)\right)^{-1} \left[\sum_r f_r \left(1 + \beta_0^{est}\left(\frac{g_r}{g_0} - 1\right)\right)^{-1}\right]^{-1} \tag{17}$$

Following the chosen Mori-Tanaka approximation, we let $k_0 = k_M$ and $g_0 = g_M$ in (15), (16) and (17).

2.3 Homogenization of poroelastic properties I: Drained stiffness and Biot coefficients

Homogenization methods for elastic and thermoelastic properties of composite materials have been around for quite some time (see review in [24]). By contrast, upscaling

of poromechanics properties is more recent [38, 39]. The most recent contribution to micro-poromechanics is due to Dormieux and co-worker (see *e.g.* [21-23]), on which we base our derivations of the poroelastic properties of cement-based materials. Like in classical continuum micro-(solid)mechanics, the (total) macroscopic stress $\boldsymbol{\Sigma}$ and the microscopic stresses $\sigma = \sigma(\mathbf{x})$ are related by the volume averaging condition:

$$\boldsymbol{\Sigma} = \langle \sigma(\mathbf{x}) \rangle_V \tag{18}$$

If the microscopic stress is of the form:

$$\sigma(\mathbf{x}) = \mathbb{C}(\mathbf{x}) : \varepsilon(\mathbf{x}) + \sigma^p(\mathbf{x}) \tag{19}$$

it is well established now (see *e.g.* [24]) that the volume average over an r.e.v. V subjected to regular boundary conditions (7), for which the classical strain localization condition of linear continuum micromechanics (8) apply, entails the macroscopic stress equation of state:

$$\boldsymbol{\Sigma} = \mathbb{C}_{\text{hom}} : \mathbf{E} = \boldsymbol{\Sigma}^p \tag{20}$$

together with the upscaling rules for the elastic stiffness $\mathbb{C}(\mathbf{x}) \rightarrow \mathbb{C}_{\text{hom}}$, and the prestress $\sigma^p(\mathbf{x}) \rightarrow \boldsymbol{\Sigma}^p$:

$$\mathbb{C}_{\text{hom}} = \langle \mathbb{C}(\mathbf{x}) : \mathbb{A}(\mathbf{x}) \rangle_V \tag{21}$$

$$\boldsymbol{\Sigma}^p = \langle \sigma^p(\mathbf{x}) : \mathbb{A}(\mathbf{x}) \rangle_V \tag{22}$$

Relation (21) is the standard expression of solid continuum micromechanics, while relation (22) is known as Levine's theorem (cited from [24]).

In the case of a poroelastic material, the macroscopic prestress $\boldsymbol{\Sigma}^p$ is linearly linked to the (average) fluid pressure, through the 2nd order tensor of Biot coefficients $\mathbf{b}$, *i.e.* $\boldsymbol{\Sigma}^p = -\mathbf{b}p$. In turn, the microprestress in such a material is the microscopic (thermodynamic) fluid pressure in the porosity, $\sigma^p(\mathbf{x}) = -\eta p \mathbf{1}$, where $\eta = 0$ in any solid phase, and $\eta = 1$ in the porosity $\phi_0 = \langle \eta \rangle_V$. In this case, for $p = 0$, which corresponds macroscopically to drained conditions, and which is equivalent microscopically to a porous material emptied of the fluid phase, the drained stiffness tensor is obtained from:

$$p = 0; \mathbb{C}_{\text{hom}} = \sum_{r=1}^{n} f_r \mathbb{C}_r \langle \mathbb{A} \rangle_{V_r} \tag{23}$$

where $\langle \mathbb{A} \rangle_{V_r}$ is the volume average of the strain localization tensor over the solid phase V_r. In the (local and global) isotropic case, for which $\langle \mathbb{A} \rangle_{V_r}$ is defined by (11), the drained bulk and shear moduli are obtained in the form:

$$p = 0 : \begin{cases} K_{\text{hom}} = \sum_{r=1}^{n} f_r k_r A_r^v \\ G_{\text{hom}} = \sum_{r=1}^{n} f_r g_r A_r^d \end{cases} \tag{24}$$

The strain localization coefficients A_r^v and A_r^d are suitably estimated by (16) and (17).

In turn, the upscaling rule (22) provides the following expression of the tensor of Biot coefficient [21]:

$$\mathbf{b} = \mathbf{1} : \phi_0 \langle \mathbb{A} \rangle_{V_{fl}} \tag{25}$$

which simplifies in the isotropic case to:

$$b = \phi_0 A_{fl}^v \tag{26}$$

where $\langle \mathbb{A} \rangle_{V_{fl}}$ is the volume average of the strain localization tensor associated with the empty pore space, and A_{fl}^v the associated volumetric strain localization coefficient. It is readily shown that (26) reduces to the classical Biot-Willis expression (3_1) for a two phase material composed of a solid and the pore space. Indeed, using the compatibility condition (9) for a two phase solid-porosity material:

$$(1 - \phi_0) A_s^v + \phi_0 A_{fl}^v = 1 \tag{27}$$

we obtain with the help of (26):

$$K_{\text{hom}} = (1 - \phi_0) A_s^v k_s = (1 - b) k_s \tag{28}$$

which is (3_1). On the other hand, it is also readily understood that the previous expression does not hold for the case of a porous material composed of several solid phases, for which the general expression (25) needs to be employed. In this case, using the compatibility conditions (9) and (10), the Biot coefficient tensor can be rewritten in the form:

$$\mathbf{b} = \mathbf{1} : \left(\mathbb{I} - \sum_{r=1}^{n} f_r \langle \mathbb{A} \rangle_{V_r} \right) \tag{29}$$

2.4 Homogenization of poroelastic properties II: Biot moduli and undrained stiffness

The drained stiffness $\mathbb{C}_{\text{hom}}$ and the Biot coefficients $\mathbf{b}_{\text{hom}}$ are necessary quantities to translate the effect of a pressure in the pore space into macroscopically effective stress-strain relation, *i.e.* Equation (1). But they are only one part of the picture of the poroelastic constitutive behavior of porous materials; the second degree of freedom of a porous material being the pressure-porosity state equation (2), which generalizes to:

$$(\phi - \phi_0) = \mathbf{b} : \mathbf{E} + \frac{p}{N} \tag{30}$$

where N is the skeleton Biot modulus. The macroscopic poroelastic state equation displays that the change in porosity $\phi - \phi_0$ can be viewed as the superposition of two macroscopic load cases to which an r.e.v. is subjected [21]; see Fig. 3:

- The first load case (denoted by a superscript $()'$) is an r.e.v., emptied of the fluid phase, $p = 0$, that is subjected at its boundary to the regular boundary condition (7), and for which the classical strain localization condition of continuum micromechanics (8) applies. It is the load case, which delivers the drained stiffness properties and

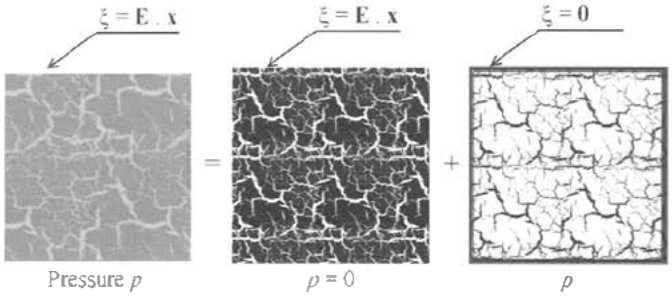

Fig. 3 - Micro-poroelasticity viewed as a superposition of an emptied poroelastic r.e.v. and a pressurized r.e.v. (adapted from [21]).

the tensor of Biot coefficient. Indeed, for this sub-problem, the volume balance of the empty porous material together with the consistency condition (9) delivers the change in porosity in the form:

$$\begin{aligned}\left(\phi-\phi_0\right)' &= \mathbf{1}:\left\langle \eta\varepsilon\right\rangle_V = \phi_0\mathbf{1}:\left\langle\varepsilon\right\rangle_{V_{fl}} \\ &= \phi_0\mathbf{1}:\left\langle\mathbb{A}\right\rangle_{V_{fl}}:\mathbf{E}\end{aligned} \tag{31}$$

A comparison with the macroscopic poroelastic state equation (30) for $p = 0$ delivers (25).

- The second load case (denoted by a superscript $()^{''}$) is the r.e.v. subjected at its boundary to a zero displacement, thus $\mathbf{E} = 0$, in which the solid-fluid interface is subjected to the fluid pressure;

$$\text{on } \partial V_{fl}: \sigma''\cdot\mathbf{n} = -p\mathbf{n} \tag{32}$$

where $\mathbf{n}$ denotes the unit outward normal to the solid phase. For this load case, we link stress and strain volume averages with macroscopic state equations. More precisely, combining (18) and (20), we obtain:

$$\mathbf{E}=0;\ \left\langle\sigma''\right\rangle_V = \sum_{r=1}^{n} f_r\left\langle\sigma''\right\rangle_{V_r} - \phi_0 p\mathbf{1} \equiv -p\mathbf{b} \tag{33}$$

or equivalently, using (29):

$$\begin{aligned}&p[\mathbf{b}-\phi_0\mathbf{1}] = p\mathbf{1}:\sum_{r=1}^{n} f_r(\mathbb{I}-\left\langle\mathbb{A}\right\rangle_{V_r}) = \\ &-\sum_{r=1}^{n} f_r\left\langle\sigma''\right\rangle_{V_r} \Rightarrow \left\langle\sigma''\right\rangle_{V_r} = p\mathbf{1}:(\left\langle\mathbb{A}\right\rangle_{V_r}-\mathbb{I})\end{aligned} \tag{34}$$

where $\left\langle\sigma''\right\rangle_{V_r}$ is the volume average over the solid volume V_r of the stresses prevailing in the solid phase $r = 1...n$. Analogously, combining the volume balance of the porous material, $\mathbf{E}=0 \Leftrightarrow \phi_0\left\langle\varepsilon''\right\rangle_{V_{fl}} = -\sum_{r=1}^{n} f_r\left\langle\varepsilon''\right\rangle_{V_r}$, with the macroscopic state equation (30) yields:

$$\begin{aligned}&\mathbf{E}=0;(\phi-\phi_0)'' = \mathbf{1}:\left\langle\eta\varepsilon''\right\rangle_V = \\ &-\mathbf{1}:\sum_{r=1}^{n} f_r\left\langle\varepsilon''\right\rangle_{V_r} \equiv \frac{p}{N}\end{aligned} \tag{35}$$

or equivalently, given the elastic nature of the solid phases, *i.e.* $\left\langle\varepsilon''\right\rangle_{V_r} = \mathbb{C}_r^{-1}:\left\langle\sigma''\right\rangle_{V_r}$:

$$\mathbf{E}=0;(\phi-\phi_0)'' = -\mathbf{1}:\sum_{r=1}^{n} f_r\mathbb{C}_r^{-1}:\left\langle\sigma''\right\rangle_{V_r} \equiv \frac{p}{N} \tag{36}$$

Finally, substituting (34) in (36), we obtain the following general expression of the skeleton Biot modulus for a porous material composed of a pore space and n solid phases:

$$\frac{1}{N} = \mathbf{1}:\sum_{r=1}^{n} f_r\mathbb{C}_r^{-1}:(\mathbf{1}:(\mathbb{I}-\left\langle\mathbb{A}\right\rangle_{V_r})) \tag{37}$$

which reduces in the isotropic case to:

$$\frac{1}{N} = \sum_{r=1}^{n}\frac{f_r(1-A_r^v)}{k_r} \tag{38}$$

The previous expression reduces to the classical expression (3_2) ($N = k_s/(b-\phi_0)$) for $n = 1$.

Last, it is useful to provide the link with the undrained poroelastic properties, by introducing the mass content currently contained in the porosity [1, 2]:

$$m = \rho_f^{fl}\phi \tag{39}$$

where ρ_f^{fl} is the current fluid mass density, which is a function of the fluid pressure, *e.g.* in the linear case:

$$\frac{\rho_f^{fl}}{\rho_0^{fl}} = 1+\frac{p}{K_{fl}} \tag{40}$$

with K_{fl} the fluid bulk modulus (K_{fl} = 2.3 GPa for bulk water), and ρ_0^{fl} the reference fluid mass density. Use of (39) and (40) in (20) and (30) yields the linearized poroelastic state equations in the form:

$$\Sigma = \mathbb{C}_{hom}^{u}:\left(\mathbf{E}-\mathbf{B}\frac{m-m_0}{\rho_0^{fl}}\right) \tag{41}$$

$$\frac{m-m_0}{\rho_0^{fl}} = \mathbf{b}:\mathbf{E}+\frac{p}{M} \tag{42}$$

where $\mathbb{C}_{hom}^{u}$ is the undrained stiffness tensor, M the Biot modulus of the entire porous material (solid + fluid phase), and $\mathbf{B}$ the 2nd order tensor of Skempton coefficients, which characterize the undrained behavior of poroelastic materials:

$$\begin{aligned}&\mathbb{C}_{hom}^{u} = \mathbb{C}_{hom}+M\mathbf{b}\otimes\mathbf{b};\ \frac{1}{M}=\frac{1}{N}+\frac{\phi_0}{K_{fl}}; \\ &\mathbf{B} = M(\mathbb{C}_{hom}^{u})^{-1}:\mathbf{b}\end{aligned} \tag{43}$$

In the isotropic case, $\mathbb{C}_{hom}^{u} = 3K_{hom}^{u}\mathbb{J}+2G_{hom}\mathbb{K}$ and $\mathbf{B} = B\mathbf{1}$, with

$$K^u_{\text{hom}} = K_{\text{hom}} + Mb^2; B = \frac{Mb}{K^u_{\text{hom}}} \tag{44}$$

2.5 Homogenization of poroelastic properties III: The case of a porous matrix

One situation that deserves special attention, since it is not explicitly captured by the standard microporomechanics theory, is the case of a composite material composed of a porous matrix and non-porous solid phases, the porosity taking effect at much smaller length scales than the one that characterize the matrix within the r.e.v. In this case, the matrix prestress is $\sigma^p(\mathbf{x}) = -b(\mathbf{x})p$. While the drained stiffness properties are still given by (23), application of Levine's theorem (22) yields:

$$\mathbf{b}_{\text{hom}} = \left\langle \mathbf{b}(\mathbf{x}) : \mathbb{A}(\mathbf{x}) \right\rangle_V \tag{45}$$

It is readily shown that (45) reduces to (25) in the case of a porous materials in which the pore space manifests itself as an identifiable morphological unit within the r.e.v., for which $\mathbf{b}(\mathbf{x}) = \eta \mathbf{1}$, $\eta = 0$ in any solid phase, and $\eta = 1$ in the porosity $\phi_0 = \langle \eta \rangle_V$. This consideration also allows one to address more complicated situations, in which the porosity manifests itself at multiple scales that are separated by more than one length scale, and in which the same pressure prevails in the fluid phases at multiple scales, *i.e.* drained conditions. Such a situation calls for a multiple step homogenization procedure.

Alternatively, (45) can be derived from a generalization of (31). Indeed, for $p = 0$, evoking the micro-to-macro strain compatibility (9) at multiple scales yields:

$$\left(\phi - \phi_0\right)' = \sum_{r=1}^{n} f_r \mathbf{1} : \left\langle \eta \varepsilon' \right\rangle_{V_r} = \sum_{r=1}^{n} f_r \mathbf{b}_r \left\langle \varepsilon' \right\rangle_{V_r} =$$
$$\sum_{r=1}^{n} f_r \mathbf{b}_r : \left\langle \mathbb{A} \right\rangle_{V_r} : \mathbf{E} \equiv \mathbf{b}_{\text{hom}} : \mathbf{E} \tag{46}$$

Analogously, for $\mathbf{E} = 0$, using (35), we obtain:

$$\left(\phi - \phi_0\right)'' = \sum_{r=1}^{n} f_r \mathbf{1} : \left\langle \eta \varepsilon'' \right\rangle_{V_r} =$$
$$\sum_{r=1}^{n} f_r \frac{p}{N_r} \equiv \frac{p}{N_{\text{hom}}} \Rightarrow \frac{1}{N_{\text{hom}}} = \sum_{r=1}^{n} \frac{f_r}{N_r} \tag{47}$$

where $1/N_r$ is defined by (37) for each porous material subsystem. Finally, a superposition of (46) and (47) yields (30), in which the contribution of each porous subsystem is such that the pore pressure prevailing in the different pore spaces remains the same:

$$\phi - \phi_0 = \sum_{r=1}^{n} f_r \left(\phi - \phi_0\right)_r =$$
$$\sum_{r=1}^{n} f_r \left(\mathbf{b}_r : \left\langle \mathbb{A} \right\rangle_{V_r} : \mathbf{E} + \frac{p}{N_r} \right) \tag{48}$$

In this case, the undrained properties are still defined by (43).

3. POROELASTIC PROPERTIES OF CEMENTITIOUS MATERIALS AT MULTIPLE SCALES

3.1 Materials: volume fractions and porosity

The materials we consider here are a cement paste and mortar prepared at a water:cement ratio of $w/c = 0.5$, using an ordinary Type I Portland cement. The mortar composition is characterized by a water-cement-sand mass ratio of $w/c/s = 1/2/4$, using a fine Nevada sand of density $\rho_I = 2{,}650$ kg/m^3, $d_{60} = 0.23$ mm and $d_{30} = 0.17$ mm. These materials have been under investigation at MIT for several years, and is well characterized by mechanical testing at multiple scales, from nanoindentation [25, 19], ultrasonic measurements of the elastic properties [25, 26], to triaxial strength and deformation properties [9, 40, 34, 41], and creep properties [42].

From mass density measurements of the hardened cement paste and mortar (see Table 3), it is possible to determine the sand inclusion volume fraction (level III):

$$\rho^* = \langle \rho \rangle_V \Leftrightarrow f_I = \frac{\rho^* - \rho^M}{\rho^I - \rho^M} = 0.36 \pm 0.03 \tag{49}$$

where ρ^M stands for the density of the porous matrix (cement paste, level II), and ρ^* for the density of the inclusion-matrix composite (mortar, level III). The obtained values are consistent with mass measurements of saturated and oven dried specimens which yield (see Table 3):

$$f_I = 1 - \frac{\Delta m^*}{\Delta m^M} = 0.31 \pm 0.03 \tag{50}$$

where Δm^* and Δm^M represent the change in mass content due to drying of the composite (mortar) and porous matrix (cement paste), respectively:

$$\frac{\Delta m^*}{\rho_0^{fl}} = \frac{M^*_{sat} - M^*_{dry}}{\rho_0^{fl} V}; \frac{\Delta m^M}{\rho_0^{fl}} = \frac{M^M_{sat} - M^M_{dry}}{\rho_0^{fl} V} \tag{51}$$

where V stands for the specimen volume, $M^*_{sat} = \rho^*_{sat} V$, $M^M_{sat} = \rho^M_{sat} V$, and where $M^*_{dry} = M^M_{dry}$ for the actual measured masses of the saturated and dried materials, and $\rho_0^{fl} = 1{,}000$ kg/m^3 is the water mass density.

Relations (50) and (51) are based on the premise that the mass change results from drying of all the water that is present in the porous matrix (incl. water in nanoporosity, gel porosity and macroporosity), when the specimen is oven dried at 105°C. It is tempting to relate the change in mass content to the porosity at different scales. For a saturated hardened cement paste of $w/c = 0.5$, for which all clinker phases have been consumed in the hydration reactions, the total mass measured is the sum of its components: C-S-H matrix, Portlandite crystals (CH) and water in the macroporosity; thus:

$$\frac{M_{sat}^{M}}{\rho_0^{fl} V} = \left(\bar{\rho}_{sat}^{LD} f_{LD} + \bar{\rho}_{sat}^{HD} f_{HD}\right) f_{CSH} + \bar{\rho}^{CH} f_{CH} + \phi_0 \quad (52)$$

where $\bar{\rho}_{sat}^{LD} = 1.93$ [29], $\bar{\rho}_{sat}^{HD} = 2.13$ [29], $\bar{\rho}^{CH} = 2.24$ are the intrinsic mass densities of the (saturated) low-density C-S-H, the (saturated) high-density C-S-H, the Portlandite, normalized by the one of water (see Table 1).

Analogously, for the dried cement paste:

$$\frac{M_{dry}^{M}}{\rho_0^{fl} V} = \left(\bar{\rho}_{dry}^{LD} f_{LD} + \bar{\rho}_{dry}^{HD} f_{HD}\right) f_{CSH} + \bar{\rho}^{CH} f_{CH} \quad (53)$$

where $\bar{\rho}_{dry}^{LD} = 1.44$ [29] and $\bar{\rho}_{dry}^{HD} = 1.75$ [29] are the normalized mass density of the dried LD-C-S-H and the HD-C-S-H (see Table 1). The difference in mass density between the saturated and the dried C-S-H phases is due to the water in both the nanoporosity and the gel porosity:

$$\bar{\rho}_{sat}^{J} - \bar{\rho}_{dry}^{J} = \varphi_0 (1 - \phi_0^J); J = LD, HD \quad (54)$$

with

$$\bar{\rho}_{dry}^{J} = \bar{\rho}_s (1 - \varphi_0)(1 - \phi_0^J) \quad (55)$$

where $\bar{\rho}_s = 2.8$ [29] is the normalized mass density of the solid building block of the C-S-H; $\varphi_0 = 0.18$ is the nanoporosity [29], $\phi_0^{LD} = 0.37$ and $\phi_0^{HD} = 0.24$ are the intrinsic porosities of the low density and the high density C-S-H phase (see Table 1). Finally, using (52) and (53) in (51), together with (54), yields:

$$\frac{\Delta m^{M}}{\rho_0^{fl}} = [\left(\varphi_0 (1 - \phi_0^{LD}) + \phi_0^{LD}\right) f_{LD} + \left(\varphi_0 (1 - \phi_0^{HD}) + \phi_0^{HD}\right) f_{HD}] f_{CSH} + \phi_0 \quad (56)$$

Equations (52) and (56) and the compatibility condition, $f_{CSH} + f_{CH} + \phi_0 = 1$ form a closed set of equations for the determination of the unknown volume fractions of the cement paste. However, this system of equations is very sensitive to small variations. It is, therefore, more appropriate to proceed in a step-to-step fashion, by starting with known volume fractions. The volume fraction of Portlandite can be easily estimated from the cement composition, here $f_{CH} \simeq 0.11$ (see Appendix); and use in (52) and (56) yields estimates for the capillary porosity and the C-S-H matrix volume fraction, which are corrected to meet the compatibility condition (as specified in the Appendix); thus $\phi_0 \simeq 0.07, f_{CSH} \simeq 0.82$.

Table 1 - Intrinsic properties of cement paste and mortar constituents I

LEVEL	Density [kg/m³]		Porosity [%]	Mass content [%]	
0: C-S-H solid	ρ_{sat}	ρ_{dry}	φ_0, ϕ_0	$\frac{\Delta m}{\rho_0^{fl}}$	
Basic Building Block	2,800		–	–	[29][a]
Globules	2,480	2,300	18[b]	18	[29][a]
I: C-S-H matrix					
C-S-H$_{LD}$	1,930	1,440	37.3 ± 0.1[c]	49[d]	[29][a]
C-S-H$_{HD}$	2,130	1,750	23.7 ± 0.1[c]	38[d]	[29][a]
II: Cement paste					
C_3S-Clinker	$\rho_c \frac{m_{C_3S}}{\sum_X m_X}$ [e]		–	–	
C_2S-Clinker	$\rho_c \frac{m_{C_2S}}{\sum_X m_X}$ [e]		–	–	
C_3A-Clinker	$\rho_c \frac{m_{C_3A}}{\sum_X m_X}$ [e]		–	–	
C_4AF-Clinker	$\rho_c \frac{m_{C_4AF}}{\sum_X m_X}$ [e]		–	–	
CH	2,240		–	–	
III: Mortar					
Sand	2,650		–	–	[34]

a) Density values of C-S-H as predicted from the quantitative colloidal model of C-S-H by Jennings [28, 29];
b) Nanoporosity (intra-globules porosity) filled by structural water;
c) Gelporosity (inter-globules porosity) of low density and high density C-S-H (excluding nanoporosity);
d) Δm = change in mass content due to drying at 105°C; includes structural water in nanoporosity and bulk water in gelporosity;
e) Clinker density determined from cement density ρ_c = 3,150 kg/m³, and the mass proportions m_X) of the four clinker phases (X = C_3S, C_2S, C_3A, C_4AF) in the cement which are provided by the cement producer.

3.2 High density and low density C-S-H phase (Level '0')

We start at level '0' which is the one of the two different types of C-S-H (see Fig. 2). Both, HD and LD C-S-H are composed of a solid phase and a pore space. According to the Jennings C-S-H model [29], this solid phase ('globules') should be the same for both phases, while that what changes is only the intrinsic gel porosity defined by (4). Mechanically speaking, this implies that the stiffness properties of the solid phase should coincide; thus with the help of (24) and (28):

$$\text{in } V_J: \left\{ \begin{array}{c} K_{\text{hom}}^J = (1 - \phi_0^J) k_s A_{s,J}^v = k_s (1 - b^J) \\ G_{\text{hom}}^J = (1 - \phi_0^J) g_s A_{s,J}^d \end{array} \right\} \quad (57)$$
$$J = LD, HD$$

where k_s and g_s represent the bulk modulus and the shear modulus of the solid phase, $A_{s,J}^v$ and $A_{s,J}^d$ are strain localization factors of the solid phase. The values of k_s and g_s are still out of reach experimentally, and that what is accessible by nanoindentation are mean values of the homogenized stiffness properties, *i.e.* K_{hom}^J and G_{hom}^J. Fig. 4 displays the

histogram of Young's modulus values for a $w/c = 0.5$ cement paste [19], which gives the mean values in Table 2 (level I). As expected, because of the lower porosity of the HD-C-S-H (see Table 2), the average stiffness of the high density C-S-H is higher than the low density C-S-H having a higher porosity. While the mean Young's modulus values nicely scale with the porosity, the Poisson's ratio is rather constant for all type of cementitious materials ($\nu = 0.24$; [43]). These values serve as input for a back analysis of the solid stiffness properties k_s and g_s, using a Mori-Tanaka scheme to estimate the concentration factors. For the cement-based materials, we obtain $k_s = 31.8$ GPa, $g_s = 19.1$ GPa, which corresponds to a Young's modulus of $E_s = 47.75$ GPa, and a Poisson's ratio of $\nu = 0.25$[3].

Furthermore, use of these values in the classical estimate (3) and (43)-(44) yield the poroelastic constants of the high-density and the low-density C-S-H:

$$\begin{aligned} b^{HD} &= 0.61 \quad N^{HD} = 85.9\ \text{GPa} \\ M^{HD} &= 8.7\ \text{GPa} \quad B^{HD} = 0.24 \\ b^{LD} &= 0.71 \quad N^{LD} = 93.1\ \text{GPa} \\ M^{LD} &= 5.8\ \text{GPa} \quad B^{LD} = 0.25 \end{aligned} \tag{58}$$

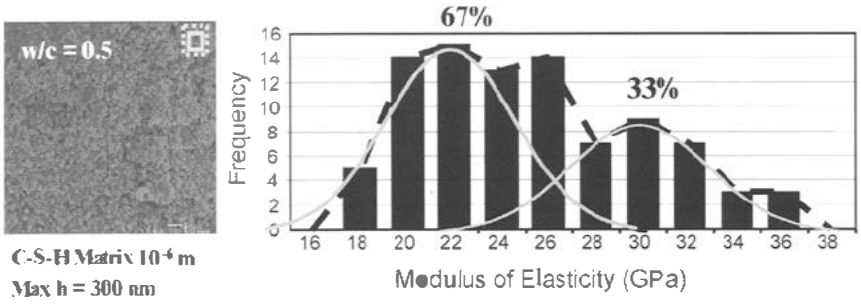

Fig. 4 - Nanoindentation stiffness measurements on a $w/c = 0.5$ cement paste. Left: C-S-H matrix with nanoindentation section. Right: Histogram of stiffness values displaying a bi-modal structure that can be associated with the two types of C-S-H, with fitted Gausian curves (adapted from [19]). The area below the curves represents the volume fractions of the high-density and low density C-S-H phases.

While it was expected that the low density C-S-H with a higher porosity has a lower Biot coefficient than the HD-C-S-H, it is interesting to note that the Skempton coefficient of both C-S-H phases is approximately the same, that is both C-S-H phase are similar sensitive to undrained loading conditions. Given the intrinsic nature of the C-S-H phases, these poroelastic constants can be considered to be universal constants for all cementitious materials.

3.3 C-S-H matrix (Level I)

The C-S-H matrix (Level I) is composed of two porous materials, the HD-C-S-H phase and the LD-C-S-H phase. The poroelastic properties of the C-S-H matrix are determined from (24), (45) and (47):

$$\text{in } V_I : \begin{cases} K^I_{\text{hom}} = \left\langle kA^v \right\rangle_{V_{CSH}} = k_{HD} + (k_{LD} - k_{HD}) f_{LD} A^v_{LD} \\ G^I_{\text{hom}} = \left\langle gA^d \right\rangle_{V_{CSH}} = g_{HD} + (g_{LD} - g_{HD}) f_{LD} A^d_{LD} \\ b^I_{\text{hom}} = \left\langle bA^v \right\rangle_{V_{CSH}} = b_{HD} + (b_{LD} - b_{HD}) f_{LD} A^v_{LD} \\ 1/N^I_{\text{hom}} = f_{LD}/N^{LD} + f_{HD}/N^{HD} \end{cases} \tag{59}$$

where we employed the consistency condition $f_{LD} A^v_{LD} + f_{HD} A^v_{HD} = 1$ and $f_{LD} + f_{HD} = 1$. Given this compatibility condition, it is readily understood that the poroelastic properties of the C-S-H matrix are all situated in between the values of the low-density and the high density C-S-H phase, *i.e.*:

$$\text{in } V_I : \left\{ \begin{array}{l} E^{LD} \le E^I_{\text{hom}} < E^{HD} \\ b^{LD} \le b^I_{\text{hom}} < b^{HD} \\ 1/N^{LD} \le 1/N^I_{\text{hom}} < 1/N^{HD} \end{array} \right\} \tag{60}$$

where $E^{LD} = 21.7$ GPa and $E^{HD} = 29.4$ GPa are the universal drained stiffness properties of the low-density and the high-density C-S-H phases, which are *directly* determined from nanoindentation (see Table 2). In between these bounds, the poroelastic properties depend on the *w/c*-ratio which affects the volume fractions f_{HD} and f_{LD} of the two types of C-S-H. These volume functions are also *directly* measurable (either by nanoindentation, see Fig. 4, or by hydration models [29, 30]). In this case, the determination of the poroelastic properties requires estimates for the concentration factors A^v_{LD} and A^d_{LD} in (59).

Using the estimate given by the Mori-Tanaka scheme, in which we choose the low density phase as matrix phase, gives:

$$A^v_{LD} = A^{v,MT}_{LD} = \frac{1 + \alpha_{LD}(\kappa - 1)}{f_{LD}[1 + \alpha_{LD}(\kappa - 1)] + f_{HD}} \tag{61}$$

$$A^d_{LD} = A^{d,MT}_{LD} = \frac{1 + \beta_{LD}(\eta - 1)}{f_{LD}[1 + \beta_{LD}(\eta - 1)] + f_{HD}} \tag{62}$$

where $\kappa = \kappa_{HD}, \eta = g_{HD}/g_{LD}$, and where α_{LD} and β_{LD} are given by (15).

The outcome of this homogenization step are the stiffness parameters of the C-S-H matrix, K^I_{hom} and G^I_{hom}, and the poroelastic constants. For a $w/c = 0.5$ cementitious material, for which $f_{LD} = 0.7$ and $f_{HD} = 0.3$, we obtain $K^I_{\text{hom}} = 15.2$ GPa and $G^I_{\text{hom}} = 9.6$ GPa, thus an elastic stiffness of $E = 23.8$ GPa, and the poroelastic constants:

$$\begin{aligned} w/c = 0.5\text{:}\ \ & b^I_{\text{hom}} = 0.69 \quad N^I_{\text{hom}} = 90.8\text{GPa} \\ & M^I = 6.4\ \text{GPa} \quad B^I = 0.24 \end{aligned} \tag{63}$$

[3] *For convenience, we recall the relation between the bulk modulus k, the shear modulus g, the Young's modulus E and the Poisson's Ratio ν:*

$$E = \frac{9g}{3 + g/k}; \nu = \frac{3 - 2g/k}{6 + 2g/k}$$

Table 2 - Intrinsic properties of cement paste and mortar constituents II: Elastic properties determined by nanoindentation.				
LEVEL	E [GPa]		ν [1]	
0: C-S-H solid				
Basic Building Block	N.A.		N.A.	
Globules	47.75	[I.A.][(a)]	0.25	[I.A.][(a)]
I: C-S-H matrix				
C-S-H$_{LD}$	21.7 ± 2.2	[25]	0.24	[43][(b)]
C-S-H$_{HD}$	29.4 ± 2.4	[25]	0.24	[43][(b)]
II: Cement paste				
C_3S-Clinker	135 ± 7	[18]	0.3	
C_2S-Clinker	140 ± 10	[18]	0.3	
C_3A-Clinker	145 ± 10	[17]	0.3	
C_4AF-Clinker	125 ± 25	[17]	0.3	
CH	38 ± 5	[25]	0.305	[35][(c)]
III: Mortar				
Sand	62.5	[34]	0.21	[34]

a) [I.A.] = determined by Inverse Analysis, includes nanoporosity (intra-globules porosity) filled by structural water;
b) Poisson's ratio estimated from comprehensive study of Le Bellego [43]);
c) CH Poisson's ratio determined by extrapolation to zero porosity [35]).

The poroelastic constants of the C-S-H matrix have been determined by a two-step homogenization procedure. Alternatively, they can be directly determined by a one-step homogenization procedure of a porous material composed of only one solid phase (of stiffness $k_s = 31.8$ GPa, $g_s = 19.1$ GPa; determined from (57), and one pore space, being defined by the C-S-H matrix porosity ϕ_0^{CSH} given in (5). The drained elastic constants are given in a similar form of (57).

Employing a Mori-Tanaka scheme, we obtain for a $w/c = 0.5$ cement paste (for which $f_{HD} = 0.3$ and $f_{LD} = 0.7$), $K^I_{\text{hom}} = 15.0$ GPa and $G^I_{\text{hom}} = 9.7$ GPa, thus an elastic stiffness of $E^I_{\text{hom}} = 23.9$ GPa; and the poroelastic constants are:

$$w/c = 0.5:\ b^I_{\text{hom}} = 0.69 \quad N^I_{\text{hom}} = 90.1 \text{ GPa}$$
$$M^I = 6.4 \text{ GPa} \quad B^I = 0.24 \qquad (64)$$

The poroelastic constants obtained with this one-step homogenization procedure compare very well with the ones determined from the two-step homogenization procedure (63). The main difference in between the two schemes is that the two-step homogenization procedure assumes the relevance of the scale separability condition at levels 0 and I (*i.e.* $(L_{HD}, L_{LD}) \gg 5.6 \times 10^{-9}$ m and $L_I \gg (L_{HD}, L_{LD})$), while the one-step homogenization procedure only assumes that the C-S-H matrix manifests itself at a length scale that is much larger than the characteristic size of the C-S-H solid phase $L_I \gg 5.6 \times 10^{-9}$ m). On the other hand, the experimental input parameters in both homogenization schemes are the same: the stiffness properties and the volume fractions of the two types of C-S-H, determined by nanoindentation (see Table 2). In the one-step homogenization procedure, the input parameters k_s and g_s are determined by a back analysis of the stiffness properties of the LD-C-S-H and the HD-C-S-H (thus assuming $(L_{HD}, L_{LD}) \gg 5.6 \times 10^{-9}$ m, which is more severe than $L_I \gg 5.6 \times 10^{-9}$ m). Hence, both upscaling schemes have similar restrictions and validity, which explain the good agreement of (63) and (64).

3.4 Cement paste (Level II)

At level II, the composite material is composed of a number of mechanically active solid phases, in addition to the porous C-S-H matrix, and an additional capillary porosity. This case if covered by (24), (45) and (47). In addition to the poroelastic properties of the C-S-H matrix, and the capillary porosity ϕ_0, the intrinsic input parameters (*i.e.* those that do not change from one material to the other) are the stiffness values of the additional solid phases (the residual clinker phases and Portlandite crystals, see Table 2).

The volume fractions of the phases are also known from mass density measurements (52) and (56). For a $w/c = 0.5$ cement paste, for which all clinker phases are consumed in the hydration reactions, the problem reduces to a composite material composed of a porous matrix (C-S-H matrix of volume fraction $f_{CSH} = V_{CSH} / V_{II} \simeq 0.82$, stiffness $k_{CSH} = K^I_{\text{hom}}$; $g_{CSH} = G^I_{\text{hom}}$), an inclusion phase (the Portlandite crystal inclusions of volume fraction $f_{CH} = V_{CH}/V_{II} \simeq 0.11$, stiffness k_{CH} and g_{CH}; see Table 2) and a macroporosity $\phi_0 \simeq 0.07$, for which:

- The drained bulk modulus and shear modulus is given by (24):

$$\text{in } V_{II}: \begin{Bmatrix} K^{II}_{\text{hom}} = f_{CSH} k_{CSH} A^v_{CSH} + f_{CH} k_{CH} A^v_{CH} \\ G^{II}_{\text{hom}} = f_{CSH} g_{CSH} A^d_{CSH} + f_{CH} g_{CH} A^d_{CH} \end{Bmatrix} \qquad (65)$$

  By estimating the concentration factors with a Mori-Tanaka scheme, the drained stiffness properties of the $w/c = 0.5$ cement paste are $K^{II}_{\text{hom}} = 14.1$ GPa, $G^{II}_{\text{hom}} = 8.7$ GPa, thus a drained Young's modulus of $E^{II}_{\text{hom}} = 21.7$ GPa. We also note that the undrained bulk modulus is $K^{u,II}_{\text{hom}} = 16.6$ GPa, and the associated Young's modulus $E^{u,II}_{\text{hom}} = 22.3$ GPa.

- The Biot coefficient is derived from (45), by adding to the Biot coefficient associated with the capillary porosity the contribution of the porous matrix:

$$\text{in } V_{II}: b^{II}_{\text{hom}} = b^{II}_0 + f_{CSH} b^I_{\text{hom}} A^v_{CSH} = \phi_0 A^v_f + f_{CSH} b^I_{\text{hom}} A^v_{CSH} \qquad (66)$$

  For the $w/c = 0.5$ cement paste, for which the capillary porosity is relatively small ($\phi_0 \simeq 7\%$), the Biot coefficient associated with this capillary porosity is small as well, $b^{II}_0 = 0.15$, and the overall Biot coefficient is dominated by the contribution of the porous C-S-H matrix, $f_{CSH} b^I_{\text{hom}} A^v_{CSH} = 0.54$; which yields a total of $b^{II}_0 = 0.69$.

- The skeleton Biot modulus is derived from (47), where we add to the contribution of the porous matrix the additional stiffness of the CH inclusion phase:

$$\text{in } V_{II}: N^{II}_{\text{hom}} = \left(\frac{f_{CSH}}{N^{I}_{\text{hom}}} + \frac{f_{CH}(1-A^{v}_{CH})}{k_{CH}} \right)^{-1} \qquad (67)$$

For the $w/c = 0.5$ cement paste, we obtain $N^{II}_{\text{hom}} = 95.5$ GPa. The overall Biot modulus is then determined from (43), by considering as effective porosity the sum of the capillary and the weighted gel porosity, *i.e.* $\phi^{II}_{\bullet} = \phi_0 + f_{CSH} \times \phi_0^{CSH}$; thus in summary for the $w/c = 0.5$ cement paste, for which $\phi^{II}_0 \simeq 0.34$:

$$\begin{aligned} &w/c = 0.5: \\ &b^{II}_{\text{hom}} = 0.69 \quad N^{II}_{\text{hom}} = 95.5 \text{ GPa} \\ &M^{II} = 5.3 \text{ GPa} \quad B^{II} = 0.22 \end{aligned} \qquad (68)$$

These results are compared with a one-step homogenization process, involving the solid phase of the C-S-H, which occupies in the cement paste the volume fraction $f^{II}_s = 1 - f_{CH} - \phi^{II}_0 = 0.55$, the total porosity of the cement paste $\phi^{II}_0 = 0.34$, and the Portlandite inclusions $f_{CH} \simeq 0.11$. Employing a Mori-Tanaka scheme (by letting $k_{\bullet} \equiv k_s = 31.8$ GPa, $g_0 \equiv g_s = 19.1$ GPa in (15), (16) and (17)), the drained stiffness properties are $K^{II}_{\text{hom}} = 14.7$ GPa, $G^{II}_{\text{hom}} = 9.1$ GPa, thus a drained Young's modulus of $E^{II}_{\text{hom}} = 22.7$ GPa, and an undrained Young's modulus of $E^{u,II}_{\text{hom}} = 23.2$ GPa; along with the poroelastic properties:

$$\begin{aligned} &w/c = 0.5: \\ &b^{II}_{\text{hom}} = 0.54 \quad N^{II}_{\text{hom}} = 161.9 \text{ GPa} \\ &M^{II} = 6.4 \text{ GPa} \quad B^{II} = 0.21 \end{aligned} \qquad (69)$$

While the stiffness properties differ little from those obtained with a multi-step homogenization procedure, the Biot coefficient is somehow lower, and the Biot skeleton modulus somehow higher. In return, the Skempton coefficient is literally the same.

3.5 Mortar and concrete (Level III)

At Level III, the material is composed of a porous matrix (the cement paste) and non-porous inclusions. From a morphological point of view, the porosity belongs to the phases at a level below (cement paste). Given the separability of scale condition, the porosity does not enter the Level III, but is already included in the poroelastic properties of the cement paste that serve as input. Consequently, the drained elastic properties are obtained from the application of (59) to the two-phase system (porous matrix and inclusions), neglecting any interface zone around the aggregates; *i.e.*:

$$\text{in } V_{III}: \left\{ \begin{aligned} K^{III}_{\text{hom}} &= k_M + (k_I - k_M) f_I A^{v}_I \\ G^{III}_{\text{hom}} &= g_M + (g_I - g_M) f_I A^{d}_I \end{aligned} \right\} \qquad (70)$$

where $k_M = K^{II}_{\text{hom}}$ and $g_M = G^{II}_{\text{hom}}$ are the elastic properties of the cement paste matrix, k_I and g_I the elastic properties of the aggregate inclusions of volume fraction $f_I = V_I / V_{III}$ given by mass density measurements (see relations (49) and (50)), while A^{v}_I and A^{d}_I are strain localization factors. For this case, the Biot parameters, b and N, are given by (45) and (47)[4]:

$$\text{in } V_{III}: \left\{ \begin{aligned} b^{III}_{\text{hom}} &= (1-f_I) A^{v}_M b^{II}_{\text{hom}} = (1 - f_I A^{v}_I) b^{II}_{\text{hom}} \\ N^{III}_{\text{hom}} &= N^{II}_{\text{hom}} / (1-f_I) \end{aligned} \right\} \qquad (71)$$

For the $w/c = 0.5$ mortar with a sand volume fraction of roughly $f_I \simeq 1/3$ (from mass density measurements (49) and (50) with values from Table 3) and known elasticity properties ($E_I = 62.5$ GPa; $\nu_I = 0.21$), we obtain $K^{III}_{\text{hom}} = 18.8$ GPa, $G^{III}_{\text{hom}} = 12.2$ GPa, thus a drained Young's modulus of $E^{III}_{\text{hom}} = 30.1$ GPa, an undrained Young's modulus $E^{u,II}_{\text{hom}} = 30.8$ GPa, along with the following poroelastic properties:

$$\begin{aligned} &w/c = 0.5: \\ &b^{III}_{\text{hom}} = 0.54 \quad N^{III}_{\text{hom}} = 143.2 \text{ GPa} \\ &M^{III} = 9.4 \text{ GPa} \quad B^{III} = 0.24 \end{aligned} \qquad (72)$$

where we employed $\phi^{III}_0 = (1-f_I)\phi^{II}_0 \simeq 0.23$ for the determination of the overall Biot modulus.

Finally, we compare these results with the ones that are obtained from a one-step homogenization procedure of a composite material, composed of three solid phases (C-S-H solid $k_s = 31.8$ GPa, $g_s = 19.1$ GPa, $f^{III}_s = (1-f_I) f^{II}_s \simeq 0.37$; Portlandite crystals $k_{CH} = 33.3$ GPa, $g_{CH} = 14.5$ GPa, $f^{III}_{CH} = (1-f_I) f_{CH} \simeq 0.07$; and sand inclusion $k_I = 35.9$ GPa, $g_I = 25.8$ GPa) and a total porosity of $\phi^{III}_0 = (1-f_I)\phi^{II}_0 \simeq 0.23$ (which includes both the gel porosity and the capillary porosity of the cement paste matrix). In this case, there is no clear dominating matrix inclusion morphology, as all (solid) phases may play the role of the matrix. This suggests the use of a self-consistent scheme for the determination of the concentration factors, *i.e.* $k_0 \equiv K^{III}_{\text{hom}}$ and $g_0 \equiv G^{III}_{\text{hom}}$ in (15), (16) and (17). This self-consistent scheme delivers slightly smaller stiffness values

---

[4] *We recall that the determination of the Biot coefficient and Biot skeleton modulus of a composite composed of a porous matrix is based on the consistency of the fluid pressure state equation. For the porous matrix:*

$$\text{in } V_M: \frac{p}{N^{II}_{\text{hom}}} = -b^{II}_{\text{hom}} E^{II} + (\phi - \phi_0)^{II}$$

where $(\phi - \phi_0)^{III}$ is the porosity change of the porous matrix, which at level III reads $(\phi - \phi_0)^{III} = (1-f_I)(\phi - \phi_{\bullet})^{II}$.

Furthermore, in the case of the empty porous matrix ($p = 0$), the strain E^{II} is related to the strain at level III by the strain localization condition $E^{II} = A^{v}_M E^{III}$. Hence, the pressure state equation at level III which is consistent with the pressure prevailing in the pore space of the porous matrix reads:

$$\frac{p}{N^{III}_{\text{hom}}} = -b^{III}_{\text{hom}} E^{III} + (\phi - \phi_0)^{III}$$

along with (71):

$$b^{II}_{\text{hom}} = (1-f_I) A^{v}_M b^{II}_{\text{hom}}; \frac{1}{N^{III}_{\text{hom}}} = \frac{1-f_I}{N^{II}_{\text{hom}}}$$

Table 3 - Measured versus predicted properties of a *w/c* =0.5 cement paste and mortar					
		LEVEL II		LEVEL III	
Measured		Cement paste $w/c = 0.5$		Mortar	
ρ_{sat}	[kg/m^3]	1,898 ± 9		2,171 ± 15	
$\frac{\Delta m}{\rho_0^{fl}}$		39.7 ± 1.1		27.5 ± 0.4	
E_{Static}	[Gpa]	18.6 ± 0.6		21.6 ± 0.4	
E_{RF}	[Gpa]	21.7 ± 0.1		25.2 ± 0.1	
E_{UPV}	[Gpa]	22.8 ± 0.5		26.5 ± 1.8	
Predicted				$f_I = 0.33$	$f_I = 0.33 \pm 0.06$
Upscaling scheme		3-step (MT)	1-step (MT)	4-step (MT)	1-step (MT)
E_{hom}	[Gpa]	21.7	22.7	30.1	28.4 ± 2.7
ν_{hom}	[1]	0.24	0.24	0.26	0.23
E^u_{hom}	[Gpa]	22.3	23.2	30.8	29.0 ± 2.6
ν^u_{hom}	[1]	0.28	0.27	0.28	0.25
b_{hom}	[1]	0.69	0.54	0.54	0.48 ∓ 0.05
N_{hom}	[Gpa]	95.5	161.9	143.2	131.7 ± 12.9
M_{hom}	[Gpa]	5.3	6.4	9.4	9.4 ± 0.9
B	[1]	0.22	0.21	0.24	0.23 ∓ 0.01

ρ_{sat} = *mass density of saturated sample;*
Δm = *change in mass content due to drying at 105°C;*
E_{static} = *Young's modulus determined from uniaxial unloading tests;*
E_{UPV} = *Young's modulus determined by Ultrasonic Pulse Velocity;*
E_{RF} = *Young's modulus determined by Resonance Frequency;*
Predicted (MT = Mori Tanaka; SCS = Self-consistent Scheme):
f_I = *sand inclusion volume fraction;*
E_{hom} = *drained Young's modulus;*
ν_{hom} = *drained Poisson ratio;*
E^u_{hom} = *undrained Young's modulus;*
ν^u_{hom} = *undrained Poisson ratio;*
b_{hom} = *Biot coefficient;*
N_{hom} = *Skeleton Biot modulus;*
M_{hom} = *overall Biot modulus;*
B = *Skempton coefficient.*

than those obtained with a multi-step homogenization procedure: $K^{III}_{hom} = 17.3$ GPa, $G^{III}_{hom} = 11.6$ GPa, thus a drained Young's modulus of $E^{III}_{hom} = 28.4$ GPa, an undrained Young's modulus $E^{u,II}_{hom} = 29.0$ GPa; and the following poroelastic properties:

$$w/c = 0.5: \quad b^{III}_{hom} = 0.48 \quad N^{III}_{hom} = 131.7 \text{ GPa} \quad M^{III} = 9.4 \text{ GPa} \quad B^{III} = 0.23 \tag{73}$$

These values are consistent with those obtained with the multi-step homogenization procedure (72), particularly the Biot modulus and the Skempton coefficient which are (almost) identical.

3.6 Discussion

The developed upscaling schemes deliver estimates of the poroelastic properties of cementitious materials at multiple scales, that are difficult to assess experimentally. Particularly, static tests in which simultaneously the mean stress and the pore pressure are monitored are difficult to perform in the purely elastic range, and involve very early on irreversible deformation. The static stiffness that is reported from such tests is often much smaller than the dynamic stiffness measured on the same material. By way of example, Table 3 reports the dynamic Young's modulus determined by Ultrasound Pulse Velocity (UPV) and Resonance Frequency (RF) of the cement paste and mortar we consider in this study, together with the static stiffness obtained from the unloading branch of a uniaxial compression test. The static modulus is some 10-20% smaller than the dynamic stiffness. Hence, a consistent comparison with the estimated stiffness values obtained by upscaling should be made with the dynamic stiffness values. More precisely,

- In UPV-tests, the stiffness is determined from the velocity with which a wave travels through the sample (for details see *e.g.* [44, 45]). Given the high frequency (in the 500 kHz - 5,000 kHz), and the associated small wave lengths on the order of 3-9 x 10^{-4} m [26], it is unlikely that liquid mass can escape the sample; and the conditions can be assumed to be undrained. Hence, UPV-measurements are suitably compared with the undrained stiffness values.
- In RF-tests, a saturated sample is brought into vibration, and the stiffness is determined from the frequency response of the sample (for details see *e.g.* [46, 47]). Given the wave lengths in the millimeter range involved, it is unlikely that the fluid pressure changes in large proportions; and the conditions can be assumed to be approximately drained. This is consistent with the general trend that RF-stiffness values are systematically smaller than UPV-measurements [48], which we also found in our study [26]; see Table 3.

Table 3 summarizes the stiffness values (and poroelastic constants) obtained by upscaling. It is interesting to note that the undrained stiffness values of the cement paste almost coincide with the UPV-stiffness ($E^{u,II}_{hom} = 22.3$-23.2 GPa versus $E^{II}_{UPV} = 22.8 \pm 0.5$); and also the drained stiffness values almost coincide with the RF-measurements ($E^{II}_{hom} = 21.7$-22.7 GPa versus $E^{II}_{RF} = 21.7 \pm 0.1$). This good agreement is a clear indication of the predictive capabilities of the homogenization scheme for the cement paste, that is the capability of the model to capture the strain localization in the solid phases. Since the strain localization is intimately related to the Biot coefficient and Biot moduli, we may interfere that the stiffness validation includes the validation of b^{II}_{hom} and N^{II}_{hom} given in (68) and (69).

By contrast, the stiffness values obtained by homogenization of the mortar with an inclusion fraction of $f_I \simeq 1/3$ are some 10-15% greater than the experimental values for both the undrained ($E^{u,III}_{hom} = 29.0$-30.8 GPa

versus $E^{III}_{UPV} = 26.5 \pm 1.8$) and the drained case ($E^{III}_{\text{hom}} = 28.4\text{-}30.1$ GPa versus $E^{III}_{RF} = 25.2 \pm 0.1$).

This is an indication of an additional micromechanical feature which adds a compliance to the composite material of non-negligible magnitude, and which has not been taken into account in our upscaling schemes. Several contributions in the open literature hint to the role of an Interfacial Transition Zone (ITZ) in between the inclusions and the cement paste matrix, which may well explain this difference. This zone is known to be a zone of on average higher porosity than the cement paste matrix. The Biot coefficient determined by neglecting the ITZ, therefore, may well appear as a lower bound of the actual Biot coefficient of the mortar. However, the difference between experimental and predicted stiffness values must also be seen in perspective of the experimental accuracy of the inclusion volume fraction determined by mass density measurements (49) and (50), *i.e.* $f_I \simeq 0.33 \pm 0.06$, in conjunction with the relatively high mortar-cement paste stiffness ratio of $E_I / E_M \approx 2.9$. Indeed, using a one-step SCS homogenization scheme, the accuracy of the determined homogenized undrained and drained stiffness is on the order of the difference between experimental and predicted values, *i.e.* $E^{u,III}_{\text{hom}} = 29.0 \pm 2.6$ GPa and $E^{III}_{\text{hom}} = 28.4 \pm 2.7$ GPa, and the associated Biot coefficient is within $b^{III}_{\text{hom}} = 0.48 \mp 0.05$ (see Table 3). In summary, while the ITZ may play a role on the poroelastic properties of mortar and concrete (particularly for very high *w/c* cement-based materials), it appears to us here (for our *w/c* = 0.5 materials) of second order compared to the sensitivity of the results with regard to the sand inclusion volume fraction.

4. CONCLUDING REMARKS

Continuum Micromechanics and advanced microstructure modeling of cement chemistry together with advanced micromechanical testing (such as nanoindentation) provide a rational means today to estimate the poroelastic properties of highly heterogeneous materials, such as cement-based materials, and to confirm that cement-based materials are poromechanics materials that are sensitive to the pressure that develops in the porosity of these materials at multiple scales.

If we admit that the gel porosity is the smallest pore space in cement-based materials in which water occurs as a bulk water phase, the poromechanical effect of this porosity dominates over capillary porosity effects. The gel porosity of 24% and 37% in high-density and low-density C-S-H, which is the same for all cement-based materials, confines the Biot coefficient within $0.61 < b^0 \leq 0.71$. Except for the case of an excessive capillary porosity, this base Biot coefficient decreases gradually at larger scales, because of the addition of non-porous solid phases (Portlandite, ..., aggregates), but is generally expected to be larger than twice the (bulk water) porosity. This relatively high value of the Biot coefficient indicates that the deformation of cementitious materials is not only governed by the deformation of the solid phases, but also by a change of the porosity, particularly of the gel porosity in the C-S-H, which is on the same order as the macroscopic deformation. In a similar way, a pressure build-up or a pressure decrease (*e.g.* capillary pressure) also entails a non-negligible change of this gel porosity, resulting in swelling or shrinkage of these materials.

The Skempton coefficient *B*, which is a measure for the sensitivity of porous material to drained and undrained conditions, is almost constant over several orders of magnitude, starting from the scale of the LD- and HD-CSH (level 0), to the scale of the cement paste (level II), and mortar or concrete composite (level III). It is on the order of $B = 0.20\text{-}0.25$, which is a rather small value for a porous material with such a high porosity. In turn, this rather small value explains the little difference between drained and undrained elastic properties, and may well explain the little consolidation effect that cement-based materials generally experience.

This may change, however, dramatically, when cementitious materials are subjected to severe chemical softening, such as calcium leaching. Calcium leaching which is one of the most severe forms of chemical softening, dissolves the Portlandite crystals and lead to a dissolution and re-precipitation of the C-S-H phases. The first lead to an increase of the capillary porosity, as the volume fraction of Portlandite becomes part of the capillary porosity; which is expected to increase the Biot coefficient of the cement paste (level II) and the mortar (level III). Furthermore, the additional dissolution and re-precipitation of the C-S-H solid phase is expected to change the base Biot coefficient b^0 (level 0) to an extent which makes cementitious materials extremely vulnerable to pressure variations in the pore space in the poroelastic domain [9]. The same holds true for poroplastic and poroviscoplastic properties of calcium leached materials, which have been addressed elsewhere [41, 42].

ACKNOWLEDGMENT

Financial support of this study by the Nuclear Energy Research Initiative of the US-Department of Energy is gratefully acknowledged. The authors also gratefully acknowledge the comments and suggestions of the Co-Guest Editor of this topical issue of *Concrete Science and Engineering*, Prof. G.W. Scherer (Princeton University). Based on his investigations of the permeability of cementitious materials [10], Scherer pointed out to us that the water in the gel porosity cannot be considered as structural water, as we assumed in the original version of this paper; and which has been reported in [34, 50]. This has been corrected in this paper and motivated the presented extension of our previous model to the nanoscale of cementitious materials (level '0').

REFERENCES

[1] Biot, M.A., 'General theory of three dimensional consolidation', *Journal of Applied Physics* **12** (1941) 155-164.

[2] Coussy, O., 'Mechanics of Porous Continua' (J. Wiley and Sons, Chichester, UK, 1995).

[3] Wittmann, F.H., 'Determination of the physical properties of cement paste', *Deutscher Ausschuss für Stahlbeton* **232**, W. Ernst and Son, Berlin, Germany (1974) 1-63 [in German].

[4] Bažant, Z.P., 'Thermodynamics of interacting continua with surfaces and creep analysis of concrete structures', *Nuclear Engrg. and Design* **20** (1972) 477-505.

[5] Wittmann, F.H., 'Creep and shrinkage mechanisms in concrete', in Z.P. Bažant and F.H. Wittmann, Editors, 'Creep and Shrinkage of Concrete' (J. Wiley and Sons, New York, 1988).
[6] Terzaghi, K., 'Principles of soil mechanics. A summary of experimental results of clay and sand', *Eng. News Rec.* (1925) 3-98.
[7] Fauchet, B., Coussy, O. Carrère, A. and Tardieu, B., 'Poroplastic analysis of concrete dams and their foundations', *Dam Engineering*, Vol. **II**(3) (1991) 165-192.
[8] Bary, B., Bournazel, J.-P. and Bourdarot, E., 'Porodamage approach applied to hydrofracture analysis of concrete', *Journal of Engineering Mechanics, ASCE* **126**(9) (2000) 937-943.
[9] Heukamp, F.H., Ulm, F.J. and Germaine, J.T., 'Mechanical properties of calcium-leached cement pastes: Triaxial stress states and the influence of the pore pressures', *Cement and Concrete Research* **31**(5) (2001) 767-774.
[10] Vichit-Vadakan, W. and Scherer, G.W., 'Measuring permeability of rigid materials by a beam-bending method: III. Cement paste', *J. Am. Ceram. Soc.* **85**(6) (2002) 1537-1544.
[11] Coussy, O., Eymard, R. and Lassabatère, T., 'Constitutive modelling of unsaturated drying deformable materials', *Journal of Engineering Mechanics, ASCE* **124**(6) (1998) 658-667.
[12] Meschke, G. and Grasberger, S., 'Numerical modeling of coupled hygromechanical degradation of cementitious materials', *Journal of Engineering Mechanics, ASCE* **129**(4) (2003) 383-392.
[13] Berryman, J.G., 'Extension of poroelastic analysis to double-porosity materials: new technique in microgeomechanics', *Journal of Engineering Mechanics, ASCE* **128**(8) (2002) 840-847.
[14] Gassmann, F., 'On the Elasticity of Porous Media', Vierteljahrsschrift der Naturforschenden Gesellschaft in Zürich 96, (1951) 1-23 [in German].
[15] Brown, R.J.S. and Korringa, J., 'On the dependence of the elastic properties of a porous rock on the compressibility of a pore fluid', *Geophysics* **40** (1975) 608-616.
[16] Rice, J.R., 'On the stability of dilatant hardening for saturated rock masses', *J. Geophys. Res.* **80** (1975) 1531-1536.
[17] Velez, K., Maximilien, S., Damidot, D., Fantozzi, G. and Sorrentino, F., 'Determination by nanoindentation of elastic modulus and hardness of pure constituents of Portland cement clinker', *Cement and Concrete Research* **31**(4) (2001) 555-561.
[18] Acker, P., 'Micromechanical analysis of creep and shrinkage mechanisms', in F.-J. Ulm, Z.P. Bažant and F.H. Wittmann, editors, 'Creep, Shrinkage and Durability Mechanics of Concrete and other quasi-brittle Materials', Cambridge, MA, August 2001 (Elsevier, Oxford UK, 2001) 15-25.
[19] Constantinides, G., Ulm, F.-J., and van Vliet, K.J., 'On the use of nanoindentation for cementitious materials', *Mater. Struct. (Special issue of Concrete Science and Engineering)* **36** (257) (April 2003) 191-196.
[20] Powers, T.C. and Brownyard, T.L., 'Studies of the physical properties of hardened Portland cement paste', *PCA Bulletin* **22** (1948).
[21] Château, X. and Dormieux, L., 'Micromechanics of saturated and unsaturated porous media', *Int. J. Numer. Anal. Meth, Geomech.* **26** (2002) 830-844.
[22] Dormieux, L., Molinari, A. and Kondo, D., 'Micromechanical approach to the behaviour of poroelastic materials', *Journ. Mechanics and Physics of Solids* **50** (2002) 2203-2231.
[23] Dormieux, L. and Bourgeois, E., 'Introduction à la micromécanique des milieux poreux' (Presses de l'École Nationale des Ponts et Chaussées, Paris, France, 2003).
[24] Zaoui, A., 'Continuum micromechanics: survey', *Journal of Engineering Mechanics, ASCE* **128**(8) (2002) 808-816.
[25] Constantinides, G. and Ulm, F.-J., 'The effect of two types of C-S-H on the elasticity of cement-based materials: Results from nanoindentation and micromechanical modeling', *Cement and Concrete Research* (2003) In press.
[26] Constantinides, G. and Ulm, F.-J., 'The elastic properties of calcium-leached cement pastes and mortars: a multi-scale investigation', MIT CEE Report R02-01, (SM-Dissertation), Cambridge, MA, 2002.
[27] Feldman, R.F. and Sereda, P.J., 'A new model of hydrated cement and its practical implications', *Eng. J. Can.* **53** (1970) 53-59.
[28] Tennis, P.D. and Jennings, H.M., 'A model for two types of calcium silicate hydrate in the microstructure of Portland cement pastes', *Cement and Concrete Research* **30**(6) (2000) 855-863.
[29] Jennings, H.M., 'A model for the microstructure of calcium silicate hydrate in cement paste', *Cement and Concrete Research* **30**(1) (2000) 101-116.
[30] Bernard, O., Ulm, F.-J. and Lemarchand, E., 'A multiscale micromechanics-hydration model for the early-age elastic properties of cement-based materials', *Cement and Concrete Research* (2003) In press.
[31] Garboczi, E.J., 'Computational materials science of cement-based materials', *Mater. Struct.* **26**(156) (1993) 191-195.
[32] Li, G.Q., Zhao, Y., Pang, S.S. and Li, Y.Q., 'Effective Young's modulus estimation of concrete', *Cement and Concrete Research* **29**(9) (1999) 1455-1462.
[33] Hashin, Z. and Monteiro, P.J.M., 'An inverse method to determine the elastic properties of the interphase between the aggregate and the cement paste', *Cement and Concrete Research* **32**(8) (2002) 1291-1300.
[34] Heukamp, F.H. and Ulm, F.-J., 'Chemomechanics of calcium leaching of cement-based materials at different scales: The role of CH-dissolution and C-S-H degradation on strength and durability performance of materials and structures', MIT-CEE Report R02-03 (D.Sc.-Dissertation), Cambridge, MA, 2002.
[35] Monteiro, P.J.M. and Chang, C.T., 'The elastic moduli of calcium hydroxide', *Cement and Concrete Research* **25**(8) (1995) 1605-1609.
[36] Eshelby, J.D., 'The determination of the elastic field in an ellipsoidal inclusion', Proc. R. Soc. London A 241, (1957) 376-392.
[37] Mori, T. and Tanaka, K., 'Average stress in matrix and average elastic energy of materials with misfitting inclusions', *Acta Metallurgica* **21**(5) (1973) 1605-1609.
[38] Auriault, J.-L., Sanchez-Palencia X., 'Étude du comportement macroscopique d'un milieu poreux saturé déformable', *Journal de Mécanique* **16**(4) (1977) 575-603.
[39] Thompson, M. and Willis, J.R., 'A reformulation of the equations of anisotropic poroelasticity', *J. Appl. Mech.* **58** (1991) 612-616.
[40] Ulm, F.-J., Heukamp, F.H. and Germaine, J.T., 'Residual design strength of cement-based materials for nuclear waste storage systems', *Nuclear Engrg and Design* **211**(1) (January 2002) 51-60.
[41] Heukamp, F.H., Ulm, F,-J. and Germaine, J.T., 'Poroplastic properties of calcium leached cement-based materials', *Cement and Concrete Research* **33** (8) (August 2003) 1127-1136.
[42] Bernard, O., Ulm, F.-J. and Germaine, J.T., 'Volume and deviator basic creep of calcium leached cement-based materials', *Cement and Concrete Research* **33** (8) (August 2003) 1155-1173.
[43] Le Bellego, C., 'Couplage chimie-mécanique dans les structures en béton attaquées par l'eau: étude expérimentale et analyse numérique', PhD. Dissertation, ENS de Cachan, France, 2001.
[44] 'Standard test method for pulse velocity through concrete', ASTM C597-83, 1991.
[45] 'Ultrasonic Pulse Velocity measurements', BS 1881: Part 203, 1986.
[46] 'Test method for fundamental transverse, longitudinal, and torsional frequencies of concrete specimens', ASTM C215-91, 1998.
[47] 'Recommendation for the measurements of dynamic modulus of elasticity', BS 1881: Part 209, 1990.
[48] Pundit manual, CNS Instruments Limited, 61-63 Homes Road, London, 1975.

[49] Taylor, H.F.W., 'Cement Chemistry', 2nd Edition (Thomas Telford, London, 1997).
[50] Ulm, F.-J., 'Chemomechanics of concrete at finer scales', *Mater. Struct.* **36** (August-September 2003) 426-438.

APPENDIX: DETERMINATION OF THE PORTLANDITE VOLUME FRACTION

The Appendix specifies how to determine the Portlandite volume fraction of a cement paste given the cement composition. We first note that 2 mol C_3S lead to 2.6 mol CH, and that 2 mol C_3S lead to 0.6 mol CH, *i.e.*

$$2C_3S + 10.6H \rightarrow C_{3.4}S_2H_8 + 2.6H$$
$$2C_2S + 8.6H \rightarrow C_{3.4}S_2H_8 + 0.6H$$

Thus, provided the C_2S and C_3S mass percent (mC_3S,mC_2S per mass cement) are known (which are generally provided by the cement producer), an upper bound estimate of the Portlandite volume fraction is given by:

$$f_{CH} \leq \frac{0.42\, m_{C_3S} + 0.13\, m_{C_2S}}{0.71 + 2.24\, w/c}$$

where we made use of the molar masses and densities of C_3S, C_2S and CH, and cement [49]. For the Type I Portland cement considered in this study, $m_{C_3S} = 0.53$ [g_{C_3S}/g_c] , $m_{C_2S} = 0.20$ [g_{C_2S}/g_c], which yields $f_{CH} \leq 14\%$. This value is not far away from the actual CH-content of the mix, which was found to be $f_{CH} = 11\%$.

With this value in hand, we solve simultaneously (52) and (56), *i.e.* the following system of equations:

$$\begin{pmatrix} \frac{M^M_{sat}}{\rho^{fl}_0 V} - 2.24\, f_{CH} \\ \frac{\Delta m^M}{\rho^{fl}_0} \end{pmatrix} = \begin{bmatrix} 1.93\, f_{LD} + 2.13\, f_{HD} \\ 0.48\, f_{LD} + 0.38\, f_{HD} \end{bmatrix} \begin{pmatrix} f_{CSH} \\ \phi_0 \end{pmatrix}$$

The solution yields values for the matrix volume fraction and the capillary porosity, which do not necessarily satisfy the compatibility condition, *i.e.* $f_{CSH} + \phi_0 + f_{CH} = 1 + \Delta$. The difference $\Delta \neq 0$ is a measure of accuracy of the determination process, and requires correction of the volume fractions. Given that both mass density measurements favor the matrix volume fraction, it is likely that the value of f_{CSH} is determined with higher accuracy than the value of the capillary porosity. The correction is therefore made onto the capillary porosity.